# Formation and Characterization of Novel Organodisilicate Glasses

Patrick J. Barrie,† Stuart W. Carr,‡ Duan Li Ou, and Alice C. Sullivan*

*Department of Chemistry, Queen Mary and Westfield College, Mile End Road, London E1 4NS, UK*

*Received April 25, 1994. Revised Manuscript Received November 4, 1994*[⊗]

Novel organodisilicate xerogel glasses have been prepared through sol–gel processing of several organo-bridged hexachlorodisilane compounds, namely, *p*-$(Cl_3SiCH_2)_2C_6H_4$, 1,4-$(Cl_3SiCH_2)_2$-2,5-$Me_2C_6H_2$, 1,4-$(Cl_3SiCH_2)_2$-2,3,5,6-$Me_4C_6$, and 9,10-$(Cl_3SiCH_2)_2$-anthracene. These new xerogels have been characterized by SEM, thermal analysis (TGA), nitrogen sorption measurement, and solid-state $^{13}C$ and $^{29}Si$ NMR spectroscopy. All of the materials are stable up to about 430 °C. The xerogels from *p*-$(Cl_3SiCH_2)_2C_6H_4$ have high surface areas with the bulk of the pore sizes being less than 50 Å. Xerogels derived from the precursor 1,4-$(Cl_3SiCH_2)_2$-2,3,5,6-$Me_4C_6$ are only slightly porous with low surface areas, while those from 1,4-$(Cl_3SiCH_2)_2$-2,5-$Me_2C_6H_2$ and 9,10-$(Cl_3SiCH_2)_2$-anthracene are nonporous. Low or complete absence of porosity in xerogels with more sterically hindering organic bridges may be associated with a high percentage of fully uncondensed silicon sites. The $^{29}Si$ NMR results show that the degree of condensation ranges from 55 to 75%, and decreases markedly with increased size of the organic group.

## Introduction

The formation of stable novel microporous materials is of considerable interest because of their great potential for material science applications. Silica xerogels with a range of physical and chemical properties are readily formed during sol–gel processing of tetraethylorthosilicate ($(EtO)_4Si$, TEOS) or related orthosilicates.[1] This approach has been successfully exploited to enable the manufacture of silica with a wide range of physical properties. It would be desirable to be able to form organic/inorganic composites using sol–gel approaches to give materials which exhibit physical properties between the inorganic and organic component. Approaches to the use of sol–gel methods to form such materials have been reviewed.[2] Schmidt has illustrated the effects on the physical and mechanical properties of incorporation of organic fragments $-CH_3$ and $H_2N-(CH_2)_3-$ in the silica gel matrix.[3] Of particular interest are the effects on sorption properties where the nature of host–guest interactions are substantially altered by the presence of the organic groups.

The more traditional approach to inorganic/organic composites is to have separate inorganic and polymer phases and to attempt to gel the inorganic component within the polymer matrix. It is difficult to produce homogeneous composites using this methodology.[3]

More recently several groups have focused on the use of well-defined inorganic–organic precursors with the potential of polymerisation *in situ* to give more homogeneous materials. Trifunctional organosilanes $RSiX_3$ (X = Cl, alkoxide) are normally employed in conjunction with the difunctional species $R_2SiX_2$ to generate silicone resins in controlled batch-hydrolysis processes.[4] Hydrolysis of the trifunctional monomers alone leads to gels consisting of randomly linked polycyclic cages.[5] Building blocks employed to form xerogels to date include functionalized octasilsesquioxanes[6] and a range of bis(triethoxysilyl)benzenes and alkanes.[7] The latter gave a series of well-characterized microporous xerogels.

The purpose of this paper is to describe our recent efforts to use well-defined organodisilicates to produce composite glasses with novel properties. We report the synthesis and detailed characterization of several novel organodisilicate glasses prepared from organobridged hexachlorodisilanes by sol–gel processing. The use of organobridged trifunctional disilane monomers is expected to provide a good opportunity for the formation of organodisilicate macromolecular materials with uniform distribution of the organic groups. Our choice of the organo-bridged hexachlorodisilanes $Cl_3SiCH_2C_6R_4-CH_2SiCl_3$, **(1–3)** and 9,10-$(Cl_3SiCH_2)_2$-anthracene (4) (wherein the Si-C bonds are stable at low pH and relatively high temperatures) has allowed the formation of a range of xerogels with relatively high thermal stability.

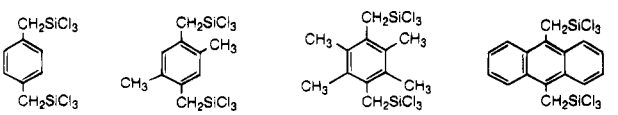


(1) (2) (3) (4)

Alkoxy functionalized silane precursors are normally used in the formation of silica or organosilicate xerogels

† Chemistry Department Christopher Ingold Laboratories, University College London, 20 Gordon Street, London WC1H OAJ, UK.

‡ Unilever Research, Port Sunlight Laboratory, Quarry Road East, Bebington, Wirral L63 3JW, UK.

⊗ Abstract published in *Advance ACS Abstracts,* December 1, 1994.

(1) Brinker, C. J.; Scherer, G. W. *Sol-Gel Science*; Academic Press: London, 1990. Day, V. W.; Klemperer, W. G.; Mainz, V. V. *J. Am. Chem. Soc.* **1985**, *107*, 8263.

(2) Novak, B. M. *Adv. Mater.* **1993**, 422–433.

(3) Schmidt, H. K. *Organically Modified Silicates as Inorganic-Organic Polymers* in *Inorganic and Organic Polymers*; Zeldin, M., Wynne, K. J., Allcock, H. R., Eds.; *ACS Symp. Ser.* **1988**.

(4) Mason, E. A. In *Silicones*; George Newnes, Ltd.: London, 1960.

(5) Frye, C. L.; Kolsowski, J. M. *J. Am. Chem. Soc.* **1971**, *93*, 4599.

(6) Agaskar, P. A. *J. Am. Chem. Soc.* **1989**, *11*, 6858.

0897-4756/95/2807-0265$09.00/0 

**Table 1. Conditions for Xerogel Formation**

| precursor | xerogel | wt (g) | THF ($cm^3$) | $H_2O$ ($cm^3$) | time (h) |
|---|---|---|---|---|---|
| 1 | X1 | 1 | 10 | 0.11 | 24 |
| 2 | X2 | 0.5 | 10 | 0.11 | 48 |
| 1 | X3 | 1 | 10 | 0.11[a] | 24 |
| 1 | X4 | 1 | 10 | 0.11 | 8[b] |
| 2 | X5 | 1 | 10 | 0.11 | 72 |
| 3 | X6 | 1 | 10 | 0.11 | 72 |
| 4 | X7 | 0.5 | 10 | 0.11 | 72 |

[a] 0.11 $cm^3$ of 1 M KOH. [b] With added 0.5 $cm^3$ of 1.23% formamide in THF solution.

as the rates of hydrolysis reactions are slower than for related chlorofunctionalized monomers, thus allowing a greater measure of control over subsequent condensation reactions. For the present work we have used chlorosilane precursors and although hydrolysis was found to occur extremely rapidly as expected, condensation at room temperature was slow, and no precipitation was observed.

## Results

**Precursor Preparation and Processing.** Synthesis and characterisation of the organobridged precursors **1**–**3** above was described in an earlier paper,[8] while those for compound **4** are given here. The conditions employed for xerogel formation are outlined in Table 1.

Time to gelation was typically 24 h for a 0.27 M THF (tetrahydrofuran) solution of precursor **1** but 48 h when the concentration was halved. Addition of catalytic amounts of formamide, a drying control agent, reduced the gel time by a factor of 3. The more highly substituted organobridged monomers **2**–**4** showed considerably longer times for gelation under similar conditions. Overall, the times for gelation, 8–24 h for **1**, were similar to those reported by Shea[7a] for similar concentrations of the related bis(triethoxysilyl)benzene under acid catalysis. It is noteworthy however that while we observed that 0.1 M solutions of 9,10-$(Cl_3SiCH_2)_2$-anthracene containing 6 mol equiv of $H_2O$ gelled after 3 days, Shea reported[7] that the analogous 9,10-$(EtO_3Si)_2$-anthracene failed to gel under acid catalysis. The gels were allowed to age for at least 24 h and the transparent glassy materials obtained were dried in air for 24 h and then under dynamic vacuum (0.001 mmHg).

**Morphology and Pore Structure.** Scanning electron micrographs of monolithic X1 revealed a granular surface with no evidence of macropore formation (Figure 1). A transparent film of X1 on glass appeared to be composed of cross-linked chains (width 50 nm) of assemblies of small particles interspersed by channels or wells of similar dimensions (Figure 2). The surface features of the film are thus quite different from those of the monolith. This may simply reflect differences in methods used for the final stages of processing (see Experimental Section).

The pore structures of X1, X3, X4, X5, X6, and X7 were examined by nitrogen gas sorption. For the purpose of this study, the xerogel samples were first ground into powders and then heated under vacuum ($10^{-3}$ Torr) at 200 °C for 48 h to remove traces of adsorbed solvents. Samples were further outgassed at 150 °C immediately prior to analysis. Equilibrium intervals of 10 s between measurements were normally used. The nitrogen sorption and desorption isotherms for X1 and X3 are shown in Figure 3 while the cumulative adsorption pore volume plots[9] are shown in Figure 4.

The sorption behavior and pore structure were very similar for the xerogels formed with added KOH or formamide. The shape of the adsorption isotherms

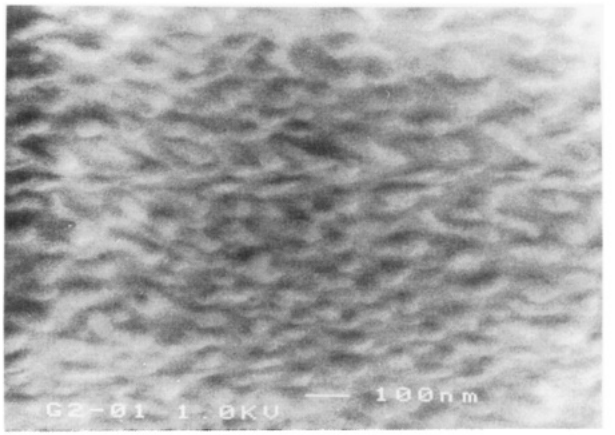


**Figure 1.** SEM of X1 monolith. Bar = 100 nm.

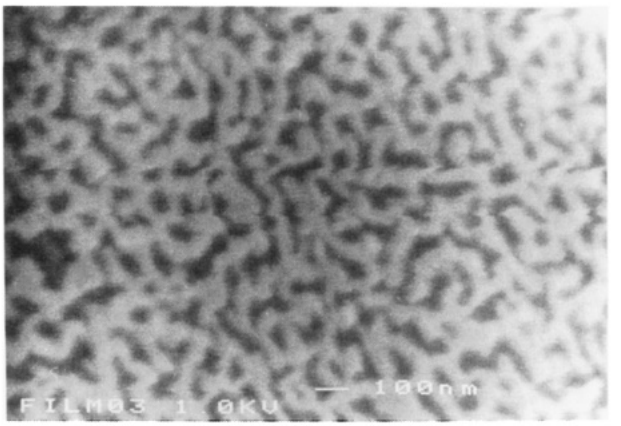


**Figure 2.** SEM of X1 film. Bar = 100 nm.

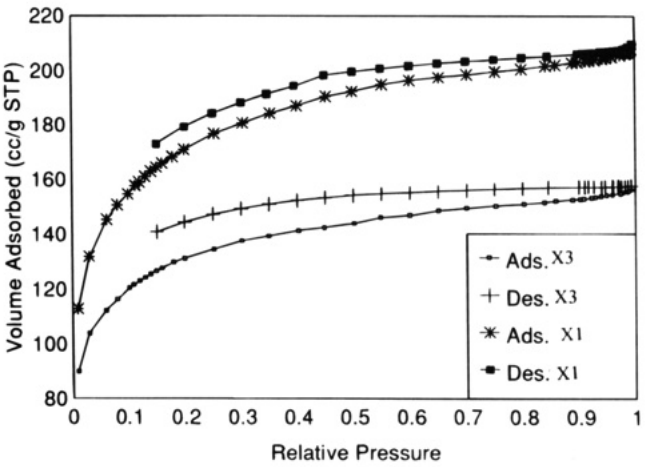


**Figure 3.** Nitrogen sorption/desorption isotherms for X1 and X3.

(7) See for example: (a) Shea, K. D.; Loy, D. A.; Webster, O. *J. Am. Chem. Soc.* **1992**, *114*, 6700. (b) Choi, K. M.; Shea, K. J. *Chem. Mater.* **1993**, *5*, 1067. (c) Oviatt, H. W.; Shea, K. D.; Small, J. H. *Chem. Mater.* **1993**, *5*, 943. (d) Loy, D. A.; Small, J. H.; Shea, K. J. *J. Non-Cryst. Solids* **1993**, *160*, 234.

(8) Carr, S. W.; Motevalli, M.; Ou, D. Li.; Sullivan, A. C. *J. Organomet. Chem.* **1993**, *445*, 35.

(9) Barrett, E. P.; Joyner, L. G.; Halenda, P. P. *J. Am. Chem. Soc.* **1951**, *73*, 373.

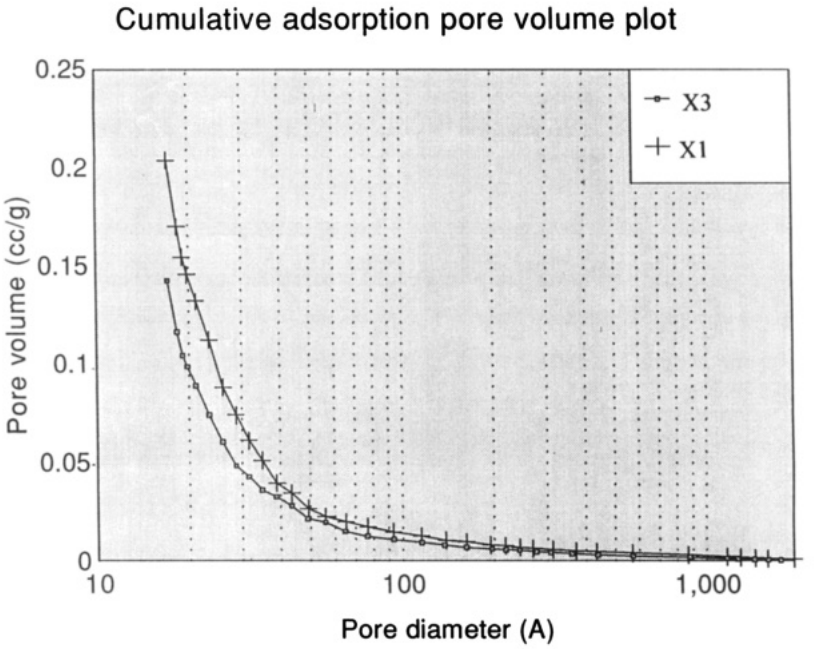


**Figure 4.** Cumulative adsorption pore volume plots for X1 and X3.

indicates that the materials contain a high proportion of relatively small pores. The adsorption/desorption hysteresis loops did not fully close for any of the samples of this series investigated. The following checks were carried out to establish the reasons behind these features of the sorption data.

(i) Analyses of X1 and X3 were undertaken wherein the equilibration interval times were increased from the normal 10 to 60 s, using the recommended tight tolerance limits allowed for deviations between measurements at each point and wherein saturation pressure was measured every 0.5 h. The shape of the resulting isotherms were unchanged, indicating that the sorption observed was for equilibrium values. The hysteresis loops remain unclosed under these conditions even at relative pressures of 0.05. Figure 5 shows the results for X3 recorded under normal and long equilibrium conditions. Figure 5a shows an expanded version of the curves in Figure 5 in the relative pressure region below $p/p_0$ values of 0.2. Figure 5b shows the sorption behavior of a sample of X1 previously heated at 300 °C and $10^{-3}$ Torr in the $p/p_0 < 0.2$ region for both normal and long equilibrium times. Both parts a and b of Figure 5 clearly show the nonclosure of the hysteresis loops at very low $p/p_0$ values.

(ii) Evacuating X1 at $10^{-3}$ Torr and 300 °C for 48 h prior to sorption analysis did not alter the shape of the isotherms (see Figure 5b) in comparison with those (Figure 3) recorded on samples evacuated at 200 °C. This indicated that the observed behavior was not due to the removal of traces of adsorbed solvent.

(iii) For sample X3 two consecutive isotherms were recorded on the same sample. Between runs of the sample was warmed to ambient to be reweighed and evacuated. The shape and nonclosure of the isotherms were the same within experimental error, indicating that the sample had not been permanently chemically or physically modified during the analysis.

(iv) Sample weight of X3 was unchanged after sorption analysis.

The nonclosure of our isotherms is a real effect and is believed to be due to the very slow desorption of $N_2$ at low $p/p_0$ pressures. It could be due to a reversible structural change leading to some poorly accessible pores from which nitrogen is not readily desorbed at 77 K.

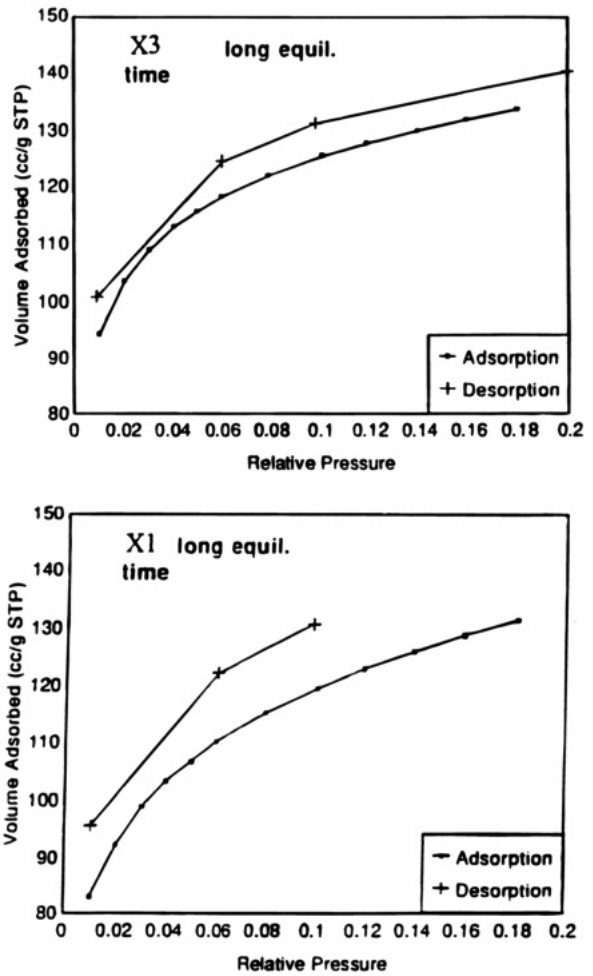


**Figure 5.** Nitrogen sorption/desorption isotherms for X3 (different equilibrium interval times). (a, top) Nitrogen sorption/desorption isotherms for X3 in $P/P_0$ region below 0.2 (b, bottom) Nitrogen sorption/desorption isotherms for X1 in $P/P_0$ region below 0.2.

**Table 2. Porosimetry Data for X1 and X3**

| xerogel | BET surface area (micropore surface area) ($m^2/g$) | BJH pore volume (micropore volume) ($cm^3/g$) | av pore diameter (Å) |
|---|---|---|---|
| X1 | 621 (608) | 0.20 (0.30) | 20 |
| X3 | 461 (452) | 0.14 (0.22) | 20 |

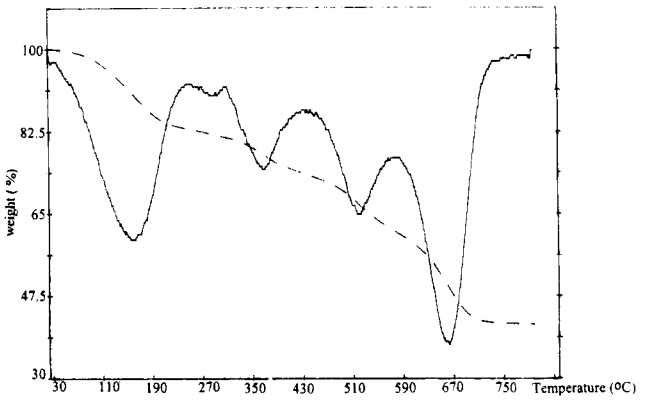


**Figure 6.** Thermogravimetric analysis curve for X1.

The BJH[9] pore size distribution plots in Figure 4 show that in both cases pore diameters range from 17 to 100 Å but more than 70% of the pores have diameters <50 Å. The BET[10] and de Boer[11] surface areas, BJH and de Boer total pore volumes, and mean pore diameters are given in Table 2. The lower surface area and total pore volume of xerogel X3 is curious, but it may be significant that this material has a substantially higher proportion of mobile uncondensed silicon environments, $T_0$ (see sections on $^{29}Si$ and $^{13}C$ solid-state NMR spectroscopy).

Of the remaining xerogels X5, X6, and X7 only X6 showed any porosity (BET area 39 $m^2/g$; BJH pore volume 0.04 $cm^3/g$), while the others were essentially nonporous (BET area < $2m^2/g$). It is noteworthy that X6 has a slightly lower proportion of $T_0$ environments than xerogel X5.

**Thermal Analysis.** Thermogravimetric profiles for the xerogels dried under vacuum at room temperature all contained similar features (Figure 6)

The peaks in the temperature range 100–200 °C are probably associated with loss of residual solvent and water. The weight loss at 300–400 °C is possibly associated with the removal of organic species trapped within the pore system or to partial dehydroxylation. Peaks above 450 °C are due to thermal degradation of the organosilicate framework, involving both Si–C and C–C bond cleavage. In support of these assignments are the $^{13}C$ and $^{29}Si$ NMR spectra of samples heated at appropriate temperatures. For example residual 1-chloro-4-butanol is removed ($^{13}C$ NMR) from samples heated at 180 °C. The percentage of $T_3$ environments increases in samples heated at 300 °C indicative of further condensation. Samples heated above 450 °C showed resonances in the $T_4$ environment which is consistent with some Si–C cleavage.

**$^{29}Si$ Solid-State NMR Spectroscopy.** Solid-state $^{29}Si$ and $^{13}C$ NMR spectra were recorded with cross-polarization (CP) and magic-angle spinning (MAS) on powdered samples of xerogels **1–4** which had been dried under vacuum at room temperature. $^{29}Si$ chemical shift data are collated in Table 3.

**Table 3. $^{29}Si$ CP MAS Chemical Shift Data ($\delta$/ppm)**

| xerogel | $T_0$ | $T_1$ | $T_2$ | $T_3$ |
|---|---|---|---|---|
| X1 | −18.0 | −53.5 | −62.0 | −71.0 |
| X2 | −19.4 | | −62.3 | −70.5 |
| X4 | −18.0 | −53.8 | −62.3 | −70.4 |
| X5 | −18.9 | −54.3 | −61.7 | −70.8 |
| X6 | −18.1 | −52.8 | −61.0 | −70.4 |
| X7 | −16.9 | | −63.6 | −71.2 |

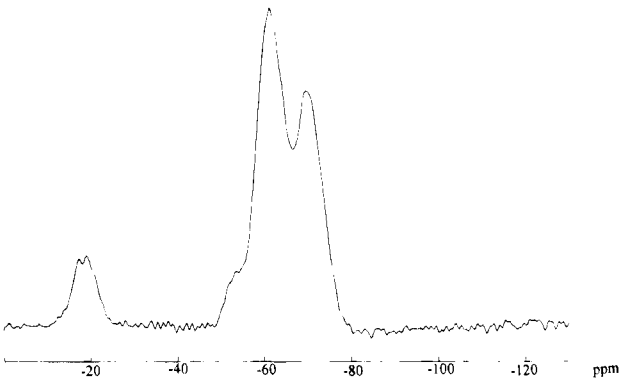


**Figure 7.** $^{29}Si$ CP MAS of X1.

The absence of any peaks in the $^{29}Si$ NMR spectrum assignable to residual Si–Cl environments (which are expected to resonate at chemical shifts greater than 0 ppm) indicates that complete hydrolysis of all samples has occurred. The presence of peaks around −54, −62, and −71 ppm, indicative of $T_1$, $T_2$, and $T_3$ groups, respectively, shows that a significant amount of silicate condensation has occurred. A broad weak peak, attributed to uncondensed $T_0$ environments, is also observed around −18 ppm in all xerogel samples, (for example see spectrum of X1 in Figure 7).

Key to $T_n$ notation and percent condensation:

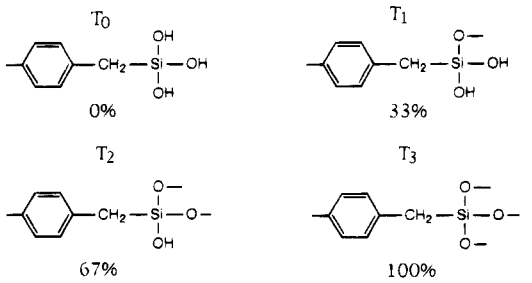


It is well-known that in $^{29}Si$ NMR the CP process is not necessarily fully quantitative as it depends on the transfer of magnetization from nearby hydrogen nuclei.[12] To correct for differences in the rate of magnetization transfer to the different sites, a variable CP contact time study was performed on sample X1, and the results are shown in Figure 8.

The curve for each environment (Figure 8) gives the best least-squares fit of the data to the equation[12]

$$I_t = I_0\{\exp(-t/T_{1\varrho}) - \exp(-t/T_{SiH})\}/(1 - T_{SiH}/T_{1\varrho})$$

The values of the CP rate, $1/T_{SiH}$, and the spin-locked relaxation time, $T_{1\varrho}$, were obtained from the variable contact time data on X1. As expected on the basis of the number of nearly hydrogen atoms, the CP rates

(10) Brunaur, S.; Emmett, P. H.; Teller, E. *J. Am. Chem. Soc.* **1953**, *60*, 309.
(11) de Boer, J. H.; Lippens, B. C. *J. Catal.* **1965**, *4*, 319.
(12) Mehring, M. *Principles of High Resolution NMR in Solids*, 2nd ed.; Springer-Verlag: Berlin, 1983.

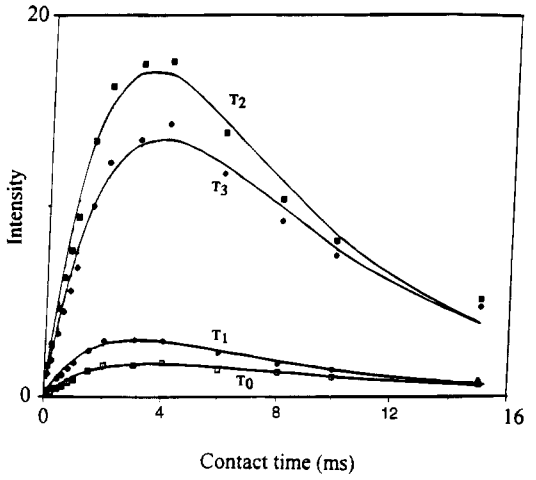


**Figure 8.** Variable contact time study for X1.

**Table 4. Relative Areas of $T_n$ Environments and Degree of Condensation Measured from $^{29}$Si CPMAS NMR Spectra**

| xerogel | $T_0$ | $T_1$ | $T_2$ | $T_3$ | % condensation |
|---|---|---|---|---|---|
| X1 | 5.2 | 5.3 | 51.3 | 38.2 | 74.2 |
| X1[a] | 4.8 | 4.8 | 50.2 | 40.1 | 75.2 |
| X3 | 9.6 | 4.0 | 50.3 | 36.1 | 71.0 |
| X5 | 11.1 | 6.1 | 58.6 | 24.2 | 65.3 |
| X6 | 7.9 | 13.7 | 62.4 | 16.0 | 62.2 |
| X7 | 33.3 | 1.8 | 31.5 | 33.5 | 55.1 |

[a] Areas corrected using $^{29}$Si cross-polarization data.

(which lie between 1.9 and 2.5 ms for $T_1$, $T_2$, and $T_3$), are in the relative order $T_1 > T_2 > T_3$ while the $T_{1\varrho}$ values for $T_1$, $T_2$, and $T_3$ sites are fairly similar. The $1/T_{SiH}$ values obtained for $T_2$ and $T_3$ are close to those observed for some pure silica gels.[13] The CP rate for $T_0$ sites is slightly slower than the $T_1$ sites, despite the larger number of hydrogen atoms in the vicinity; this may be a reflection of a higher degree of mobility for the terminal $T_0$ groups.

The $^{29}$Si CPMAS spectra allow the overall degree of condensation to be calculated for each sample using the equation

$$\text{degree of condensation} = \{0.33I(T_1) + 0.67I(T_2) + I(T_3)\}/\sum I(T_n)$$

where $I(T_n)$ represents the area under each $T_n$ peak ($n$ = 0–3). The overlapping peaks were deconvoluted assuming Gaussian peaks in order to measure the relative areas of the $T_n$ peaks and results obtained using a 2 ms contact time are shown in Table 4. The degree of condensation and relative areas of $T_n$ environments were very similar for xerogel samples dried under vacuum at room temperature and at 180 °C.

For the case of xerogel X1 the degree of condensation was calculated both using the measured areas and using areas corrected for the CP. The corrected areas give a slightly higher value for the degree of condensation than the uncorrected areas, principally due to the slight discrimination of the CP process against $T_3$ groups. The difference is only small (1.0%), so it is expected that the uncorrected areas give reasonably reliable condensation measurements for the other samples. The results in Table 4 show that the degree of condensation decreases markedly with increasing substitution of the phenyl hydrogens in $Cl_3SiCH_2C_6H_4CH_2SiCl_3$ by methyl groups. A slightly different pattern is observed for the xerogel prepared using the bulky 9,10-$(Cl_3SiCH_2)_2$-anthracene organic precursor. Here the overall level of condensation is 55.1%, but this is due principally to the large amounts of $T_0$ material remaining. A significant amount of condensation has taken place, and it is in this sample that $T_3$ sites (from complete condensation) are present in larger amounts than $T_2$ sites.

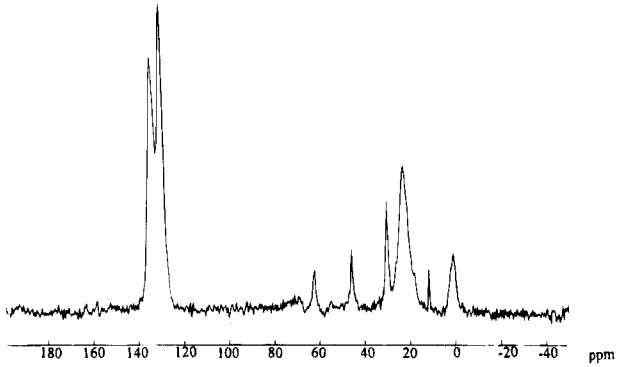


**Figure 9.** $^{13}$C MAS TOSS NMR of X1.

**Table 5. $^{13}$C CP MAS TOSS Chemical Shift Data ($\delta$/ppm)**

| xerogel | aromatic | $-CH_2-$ ($T_1 - T_3$) | $-CH_3$ | residual solvent | $-CH_2-$ ($T_0$) |
|---|---|---|---|---|---|
| X1 | 129.6, 134.1 | 22.5 | | 62.0, 45.7, 30.0 | 0.8 |
| X4 | 133.8, 129.6 | 22.5 | | 62.1, 45.6, 30.0 | 1.4 |
| X5 | 132.6 | 19.9 | 20.1 | 66.9, 45.0, 30.1 | 0.9 |
| X6 | 131.7 | 17.8 | 17.7 | 63.5, 45.0, 30.2 | 0.8 |
| X7 | 129.9, 125.9 | 15.9 | | 44.2, 29.5 | 1.3 |

There are a few recorded chemical shift positions of $RSi(OH)_3$ species in the literature; $PhSi(OH)_3$ (in solution) is known to come between −12.6 and −25.4 ppm depending on solvent.[14] Further support for the present $T_0$ assignment comes from the observation that solution NMR studies of the xerogel syntheses show the immediate formation of a species with this chemical shift position upon hydrolysis. The concentration of this species gradually decreases during condensation. It is reported that phenyl-bridged disilicates obtained on hydrolysis of bis(triethoxysilyl)benzenes show no $T_0$ species. The $T_0$ environments may result both from unreacted hydrolysed material and from groups terminating the organosilicate framework. The peak arising from the $T_0$ environment is significantly larger for the xerogel X7 synthesized using 9,10-$(Cl_3SiCH_2)_2$-anthracene from those from the other organo-bridged hexachlorodisilane starting materials. This is a consequence of the bulky anthracene unit limiting the degree of condensation.

**$^{13}$C Solid-State NMR Spectroscopy.** $^{13}$C CPMAS spectra of samples X1 and X5 are shown in Figure 9, while chemical shift data for the whole series is collated in Table 5.

Spectra were also acquired using dipolar dephasing or nonquaternary suppression[15] which has the effect of suppressing signals from those carbons with directly attached hydrogens unless the group is highly mobile. The methylene groups of the organic bridges linked to $T_1$, $T_2$, and $T_3$ sites are not resolved from each other

(13) Maciel, G. E.; Sindorf, D. W. *J. Am. Chem. Soc.* **1980**, *102*, 7606. Leonardelli, A.; Facchini, L.; Fretigny, C.; Tougne, P.; Legrand, A. P. *J. Am. Chem. Soc.* **1992**, *114*, 6412.

(14) Harris, R. K.; Mann, B. E. *NMR and the Periodic Table*; Academic Press: London, 1978.

(15) Opella, S. J.; Frey, M. H. *J. Am. Chem. Soc.* **1979**, *101*, 5854.

and give rise to a broad peak around 20 ppm. This peak does not appear in spectra recorded with 40 $\mu$s dipolar dephasing time. The methylene groups attached to $T_0$ sites give rise to a peak at 1 ppm. Surprisingly, this peak is not removed by the dipolar dephasing, indicating that these groups have a high degree of mobility. The aromatic carbons as expected appear between 126 and 134 ppm.

In addition to the resonances assigned to the organic bridges within the xerogel frameworks, the $^{13}C$ spectra of all samples showed the presence of small quantities (traces in some cases) of a mobile organic species with peaks at 29.9, 45.7, and 62 ppm in the relative ratios 2:1:1. These may be assigned to 1-chloro-4-butanol, $ClCH_2CH_2CH_2CH_2OH$, trapped in the xerogel matrices. The solution $^{13}C$ NMR spectrum of $ClCH_2CH_2CH_2CH_2OH$ has peaks at 29.4, 30.0, 45.3, and 62.3 ppm,[16] and this product may originate from HCl-promoted ring-opening of THF, the only organic solvent used in the sol–gel process. The relative intensity of peaks due to this residual solvent substantially decrease when samples are dried under vacuum at 180 °C.

## Conclusions and Future Work

Our results show that the organo-bridged hexachlorodisilane compounds **1**–**4** may be processed by sol–gel techniques to give transparent glassy materials either as thin films or monoliths. The xerogel frameworks are stable up to 430 °C. Solid-state NMR shows that despite the low pH conditions of the sol–gel process the organic bridge survives intact. The indications from porosimetry are that materials derived from precursor **1** only have significant porosity. It may be significant that these materials which have the least sterically demanding organic bridge have the highest degree of condensation as shown by analysis of the $^{29}Si$ CPMAS spectra. However it also appears to be the case that porosity depends on the number of $T_0$ groups present within the sample. This is probably because the groups arise from uncondensed material which block the porous system. Thus xerogel X6 with relative $T_0$ area of 7.9% was found to be slightly porous, while X5 which has a slightly higher overall degree of condensation and a less highly substituted aryl bridge, but a relative $T_0$ area of 11.1% was nonporous. In addition the relative areas of the $T_0$ resonances in X1 and X3 show similar correlations with porosity.

We are currently carrying out porosimetry studies on a wide range of the xerogels of the type discussed here formed from related alkoxy compounds to assess effects of precursor hydrolysable functionality on pore structure. We are also investigating the optical, catalytic, and sorption properties of xerogels doped with organic and inorganic compounds. The results of these studies will be reported in future papers.

(16) Barabas, A.; Botar, A.; Gocan, A.; Povici, N.; Hodson, F. *Tetrahedron* **1978**, *54*, 2191.

## Experimental Section

The precursors **1**–**3** above were prepared as described earlier. Standard Schlenk line techniques were employed for manipulations involving **1**–**4**. Scanning electron micrographs (SEM) were obtained using a JEOL JC6300 microscope; nitrogen sorption porosimetry was performed with a Micromeritics ASAP 2400 instrument. For thermogravimetric analysis a Perkin-Elmer TGA7 system was used. The $^{13}C$ and $^{29}Si$ NMR spectra were acquired using cross polarization (CP), magic angle spinning (MAS), and high-power proton decoupling on a Bruker MSL-300 spectrometer. Typical conditions were 2 ms contact time, 1 s recycle delay, a 90° pulse length of 4.07 $\mu$s, and a spinning speed of 4.5 kHz. Spinning sidebands in the $^{13}C$ spectra were suppressed using the TOSS pulse sequence. The $^{13}C$ and $^{29}Si$ frequencies were 75.5 and 59.6 MHz, respectively. All spectra were recorded at room temperature, and chemical shifts are quoted relative to TMS.

**9,10-($Cl_3SiCH_2$)$_2$-anthracene.** A mixture of 9,10-bis(chloromethyl)anthracene (5.5 g, 20 mmol) and trichlorosilane (6.1 cm$^3$, 60 mmol) in tri-*n*-propylamine (7.6 cm$^3$) was kept at 140–160 °C for 72 h. Addition of diethyl ether (50 cm$^3$) to the cooled mixture resulted in precipitation of the amine hydrochloride. Filtration followed by removal of solvent under vacuum afforded the product as yellow powder (6.43 g, 68%), mp >300 °C.

$^1H$ NMR (80 MHz, $CDCl_3$) $\delta$ 3.73 (s, 4H), 7.49–7.78 (m, 4H), 8.17–8.44 (m, 4H); $^{13}C$ NMR (62.89 MHz, $CDCl_3$) $\delta$ 26.31, 125.14, 125.78, 129.78; $^{29}Si$ NMR (49.66 Hz, $CDCl_3$) $\delta$ 7.04.

Mass spectrum: *m/e* (%, fragment) 469.8608 (28.7, $C_{16}H_{12}Si_2{}^{35}Cl_6$); 471.8575 (58.5, $C_{16}H_{12}Si_2{}^{35}Cl_5{}^{37}Cl$); 473.8545 (51.9, $C_{16}H_{12}Si_2{}^{35}Cl_4{}^{37}Cl_2$); 475.8517 (23.9, $C_{16}H_{12}Si_2{}^{35}Cl_3{}^{37}Cl_3$); 338.9784 (100, $C_{16}H_{12}Si_2{}^{35}Cl_5{}^{37}Cl-Si^{35}Cl_3$).

**General Procedure for Sol–Gel Processing 1–4.** A solution of the precursor in anhydrous THF, generally (1.0 g) in 10 cm$^3$, was placed in a 100 cm$^3$ Pyrex round-bottomed flask in a nitrogen atmosphere. Water (0.11 cm$^3$) was syringed into the THF solution in one go. The slightly exothermic aqueous mixture was stirred to room temperature and then allowed to stand in a static $N_2$ atmosphere until a transparent gel formed (8–72 h). Once formed, the gels were left to age for 24 h and then to dry in air for 24 h before being finally dried under dynamic vacuum (0.001 mmHg). The air-dried gels had the hemispherical shape of the round-bottomed flask. Vacuum drying was accompanied by some fracturing. Overall, drying resulted in approximately 70% shrinkage. The xerogel fragments were all transparent glassy pale yellow or pink materials. The precise formulations used in a number of experiments are given in Table 1.

A thin film of X1 was obtained by coating a glass slide with the fluid sol and subsequently allowing this to stand over THF in a sealed desiccator for 48 h and in a dynamic THF atmosphere for 4 days. The transparent film was subsequently further dried and stored in air with no observed fracturing.

**Acknowledgment.** We are grateful to Unilever Research for financial support and Wendy Whitby, Unilever Research, for porosimetry measurements; D.L.O. thanks the Airey Neave trust for financial assistance. The solid-state NMR spectra were recorded by the University of London Intercollegiate Research Facility at University College London.

CM940213L